

## Bidirectional AC/AC converter linking two microgrids in a flexible microgrid

Nguyen The Vinh<sup>1</sup>, Nguyen Van Dung<sup>2</sup>

<sup>1</sup>Faculty of Electronic Engineering I, Posts and Telecommunications Institute of Technology, Hanoi, Vietnam

<sup>2</sup>Faculty of Electronic Engineering, Hanoi University of Industry, Hanoi, Vietnam

### Article Info

#### Article history:

Received Oct 16, 2024

Revised Dec 2, 2024

Accepted Dec 26, 2024

#### Keywords:

AC-AC converter

Boost converter

Buck converter

Increase and decrease voltage

Micro-grid operating procedures

### ABSTRACT

The proposed single-phase flexible AC/AC converter in an AC microgrid controlled by the PWM method is presented and tested with a small capacity. This converter uses a simple and small number of semiconductor switches and passive elements to limit power loss and increase efficiency. It has higher reliability, safety, and continuity of power supply in operation than traditional AC/AC converters due to the power circuit structure of the converter. It has the function of increasing or decreasing voltage when connecting to two microgrids and can be directly connected to distributed energy sources in microgrid systems with distributed power sources and loads. Besides, the AC/AC converter can be connected to the storage system to improve continuity and voltage stability for the grid. The performance of the proposed converter is compared with existing similar converters. The paper presents the analysis of simulation results by OrCAD with power values from 0.1-5 kW and experimental power with typical values in the range of 0.5-3.5 kW at different scenarios of the converter.

*This is an open access article under the [CC BY-SA](https://creativecommons.org/licenses/by-sa/4.0/) license.*



### Corresponding Author:

Nguyen The Vinh

Faculty of Electronic Engineering I, Posts and Telecommunications Institute of Technology

Hanoi, Km.10, Nguyen Trai Street, Ha Dong District, Hanoi, Vietnam

Email: vinhnt@ptit.edu.vn

## 1. INTRODUCTION

A microgrid (MG) is a relatively small power grid system, a controllable grid consisting of one or more generating units connected to nearby users that can be operated together with or independently of the local (i.e. high voltage) transmission system, sometimes referred to as a “grid” [1]-[3]. Because energy is generated near where it is used, microgrids are a form of distributed generation [4]. When the microgrid operates in standalone mode, there are problems with nonlinear loads and power electronic converters that change the parameters in the microgrid [5]. Microgrids also have the characteristics of fast and uneven load distribution [6]. Reasons causing system instability include renewable energy sources (location, source characteristics); reactive power demand; and nonlinear electrical equipment. These types lead to voltage fluctuations, harmonics, and voltage dips/swells respectively. Several standards have been developed to address and handle these problems [7], [8]. The root mean square (RMS) voltage drop of the distribution line ranges from 90% to 10%, and the RMS voltage increases from 110% to 180% [9]. These problems can be solved by proper monitoring and suitable compensation techniques [10].

AC-to-AC converters are more complex than AC-to-DC converters because AC conversion requires changes in voltage, frequency, and bipolar voltage blocking capabilities, which often require complex device topologies [11], [12]. The pulse width for the switch limits the input power value (200 W) resulting in low experimental average efficiency [11], [12]. Another way to achieve AC/AC conversion is to use AC/DC and

DC/AC through an intermediate DC link and improve renewable energy sources' energy efficiency [8], [13]. While operating at unity power factor, the bidirectional AC-DC/DC-AC converter will rectify the active power transferred from the DC grid to the AC grid [14]. Converters in general and AC/AC converters in particular play an important role in modern power electronics systems. These converters are highly efficient in controlling AC RMS voltage and frequency in various applications [15], [16]. Power factor correction (PFC) is another common use of AC/AC converters in power distribution systems, especially large industrial and commercial applications [17], [18], where poor power factor leads to increased energy costs and possible penalties from loads (businesses or factories). By regulating the reactive power delivered to the load, these converters can reduce energy loss, maintain a power factor close to 1, and improve overall power quality [19], [20]. Uninterruptible power supply (UPS) converters ensure the efficient operation of sensitive electronic devices, such as computers, servers, and medical equipment, in the event of power quality problems, by regulating the RMS output voltage and frequency [21].

Block diagram of the system connecting AC microgrids using DC/DC, DC/AC, and AC/AC converters to flexibly distribute the grid and optimize the efficiency of distributed energy sources as shown in Figure 1. This paper proposes a flexible AC/AC converter with a simple structure and direct power transfer connecting two AC microgrids. This converter performs energy transmission processes between two grids to ensure voltage quality on the two grids, optimize operation, and improve the input efficiency of the converter and the efficiency of energy use from distributed sources through priority loads according to the conditions and regulations of Vietnam and the world [22]. The paper is structured as follows: i) Section 2 describes in detail the working principle of the proposed structure; ii) Section 3 presents the simulation results with theory to evaluate the converter performance; iii) Section 4 presents the experimental results to evaluate the converter performance and the theoretical aspects, simulation, and typical references; and iv) Section 5 concludes and summarizes the important achievements of the work in the paper.

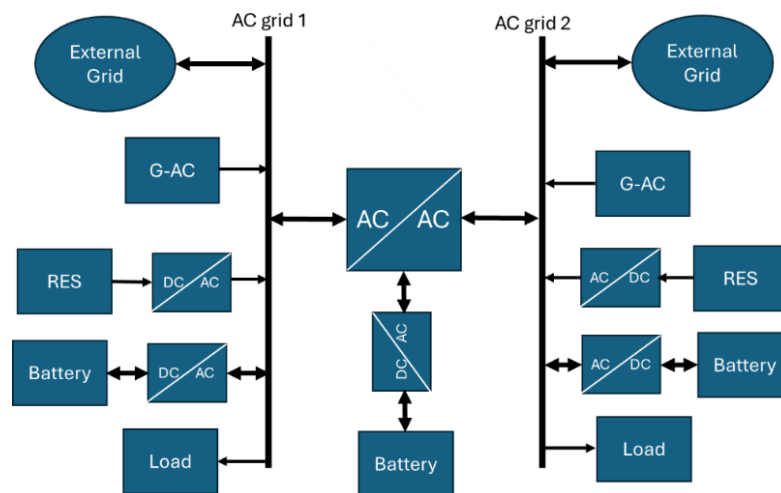


Figure 1. Block diagram of the AC microgrid connection system

## 2. FLEXIBLE AC/AC CONVERTER

Figure 2 shows the principle of a proposed bidirectional AC/AC converter circuit based on Boost and Buck. It consists of three power switches connected to a diode bridge to reduce voltage stress, two coils L1 and L2, and two LC filters on both sides connected to two grids AC1 and AC2. The power circuit of the converter represents the main switches in the circuit that perform the power conversion, the recovery circuit components and the connection to the storage system are analyzed in more detail in section 2.2 of this section. Figure 3 shows the main waveforms of the AC/AC converter operation. A power switch is activated by a high-frequency sinusoidal pulse width modulation (SPWM) during each half cycle of the input voltage. Each switching cycle has two states, as shown in Figure 3. In the main waveform graph shows the full cycle of the alternating current (2 $\pi$  cycle). Control frequency for the electronic switches M1-M3.

### 2.1. Operating principle of the converter

In this proposed converter two bidirectional switches are used which are connected in Boost and Buck form. Through the filter circuits, harmonic filtering of orders 3, 5, and 7 is performed. This converter converts

energy directly from two AC power grids, so the geographical conditions of the two grids must also be close to each other (distance 10-1000 m) [23], [24]. The switches are selected to suit the power range in the converter.

The conditions during the energy transfer between two microgrid ACs are as follows:

- Load conditions are preferential for customers from type 1 to type 3 according to Vietnam's regulations [25]. In the AC microgrid, there are practical civil and domestic loads.
- The optimal grid-independent operating conditions using renewable energy sources: in two AC grids there is a combination of renewable energy sources and storage systems.
- Level 1 priority is the loads in the 2 microgrids when the AC/AC unit proposes to connect.
- Grid-connected condition, using both load priority and AC microgrid renewable energy source working independently. For example, if transmitted from AC1 to AC2 grid.

$$P_{loadAC2} > P_{PV2} + P_{win2} + P_{source-AC2} \quad (1)$$

Where  $P_{PV2}$  is PV power capacity in the AC2 grid;  $P_{win2}$  is Win power capacity in AC2 grid;  $P_{source-AC2}$  is a power source in the AC2 grid.

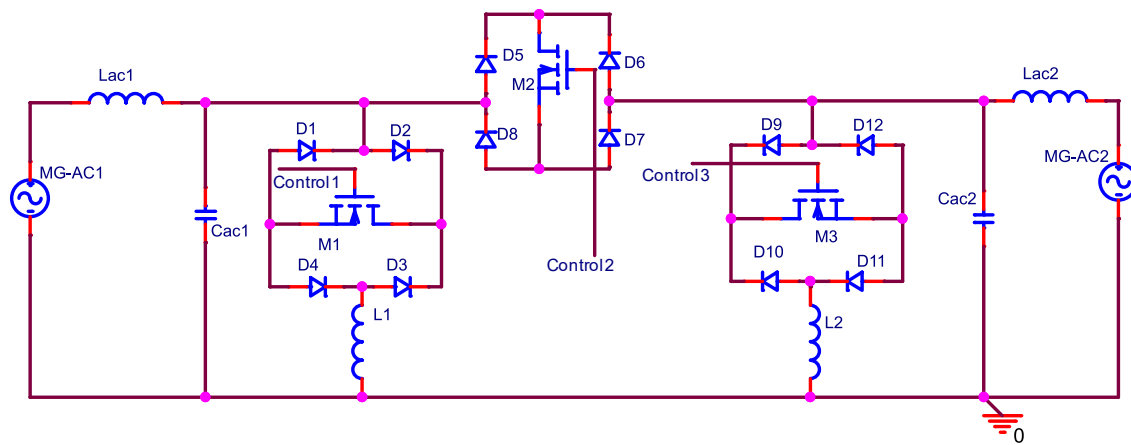


Figure 2. Circuit diagram of the proposed converter principle

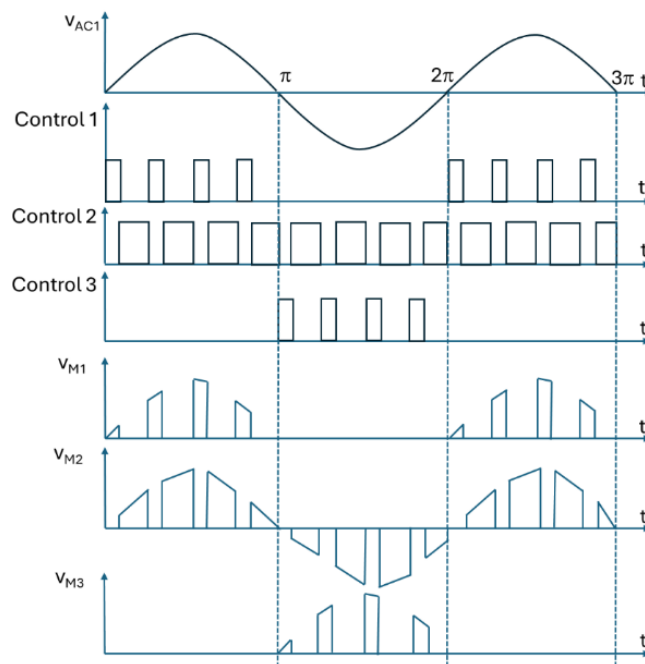


Figure 3. Basic operating diagram of the proposed AC/AC converter

In practice the Ppv and Pwin sources fluctuate instantaneously in a value that requires compensation and energy consumption.

$$P_{loadAC2} > P_{win2} + P_{source-AC2} \quad (2)$$

Ppv stops generating electricity during off-peak hours, or when the bamboo is obscured by clouds.

$$P_{loadAC2} > P_{source-AC2} \quad (3)$$

Ppv and Pwin sources do not generate energy.

### 2.1.1. Scenario one

The power transmitted from grid AC1 to AC2 in this scenario has the following modes:

a) Mode 1

Positive half cycle (0- $\pi$ ), switches M1-M3 are controlled sequentially as cases: i) Switches M1 and M2 are controlled together in a certain period of time according to the switching cycle as shown in Figure 4; ii) In the time period t1-t2 in the switching cycle M1 is turned on, M2 and M3 are turned off as shown in Figure 5; and iv) In the time period t2-t3 in the switching cycle M2 is turned on M1 and M3 are turned off as shown in Figure 6.

In Figure 4, in this half cycle, the converter power circuit performs the energy transfer process with the basic Boost circuit working principle. The power switches M1 and M2 are controlled at the same time. The energy is mainly transmitted to the AC2 grid side, and a part is dispersed to some components in the power circuit such as the coil side L1 and for Cac2. The lost energy is divided among the switching molecules M1, M2, D2, D4, D5, and D7.

The output voltage expression at grid AC2 is: Based on Kirchhoff's voltage and current laws (KVL and KCL), the instantaneous voltage and current of the inductor and capacitor are determined by (4) for the on state of M1 and M2.

$$u_{MG2} = \frac{1}{1-d1} \sqrt{2} \cdot V_{MG1} \sin \omega t \quad (V) \quad (4)$$

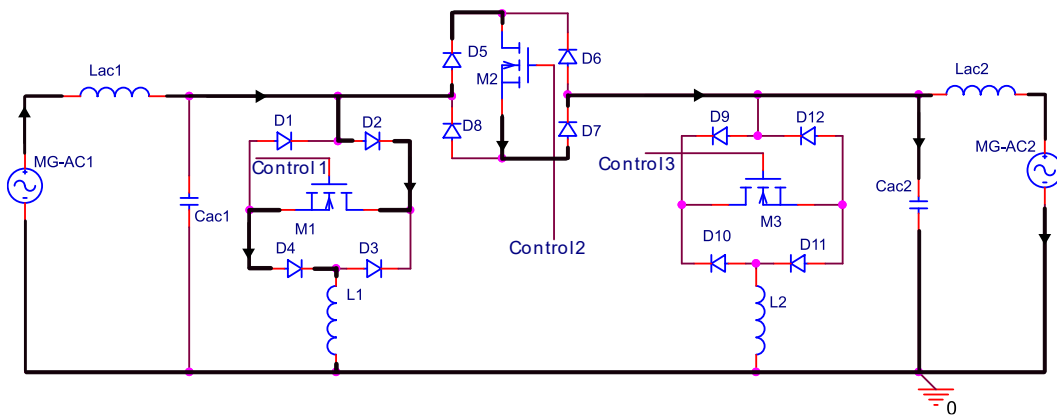


Figure 4. Status diagram of the converter operation when switches M1 and M2 are on at the same time

Figure 5 shows the operation of the converter circuit when only M1 is on. M1 has a control pulse to open. The output voltage AC2 is equal to the voltage on capacitor Cac2 and is supplied with energy from Cca2.

Expression for the state:  $u_{MG2} = u_{Cac2}$

Figure 6 describes the operation of the AC/AC power circuit when M2 is on, the energy of the AC2 grid is supplied from the AC1 grid through molecules D5, M2, and D7 the voltage expression of the AC2 grid.

$$u_{MG2} = d2\sqrt{2} \cdot V_{MG1} \sin \omega t \quad (V) \quad (5)$$

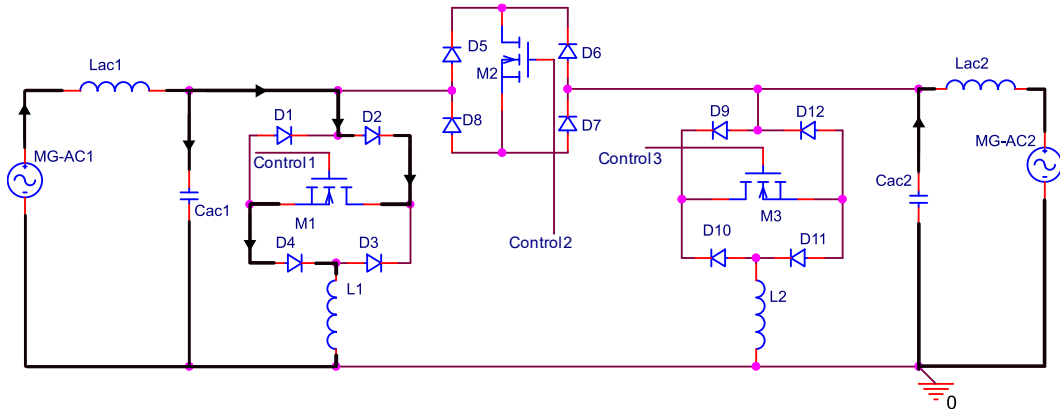


Figure 5. State diagram of converter operation when M1 is on

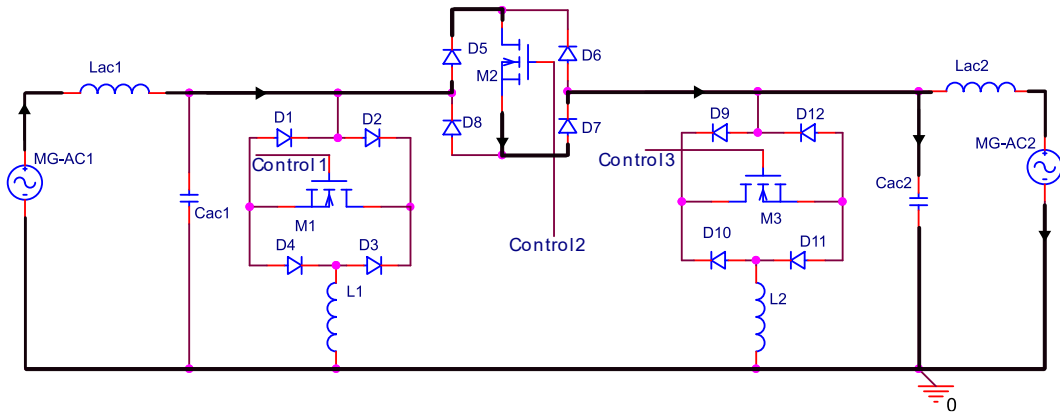


Figure 6. State diagram of converter operation when M2 is on

## b) Mode 2

Negative half cycle ( $\pi-2\pi$ ), the switches M1-M3 are controlled sequentially as in the cases: i) M2 and M3 are both controlled for a certain period of time according to the switching cycle as shown in Figure 7; ii) during the time period  $t_1-t_2$  in the switching cycle M3 is turned on in Figure 8, M1 and M2 are off; and iii) during the time period  $t_2-t_3$  in the switching cycle M2 is turned on M1 and M3 are off as shown in Figure 9.

Figure 7 describes in this half cycle; the converter power circuit performs the energy transfer process with the basic Boost circuit working principle. The power switches M2 and M3 are controlled at the same time. The energy is mainly transmitted to the AC2 grid side, and a part is dispersed to some components in the power circuit such as the coil side L2. The lost energy is divided among the switching molecules M2, M3, D6, D8, D9, and D11.

The output voltage expression at grid AC2 is: Based on Kirchhoff's voltage and current laws (KVL and KCL), the instantaneous voltage and current of the inductor and capacitor are determined by (6) for the on state of M1 and M2.

$$u_{MG2} = \frac{1}{1-d_1} \sqrt{2} \cdot V_{MG1} \sin \omega t \quad (V) \quad (6)$$

Figure 8 describes the operation of the AC/AC power circuit when M2 is on, the energy of the AC2 grid is supplied from the AC1 grid through molecules D6, M2, and D8 the voltage expression of the AC2 grid.

$$u_{MG2} = d_2 \sqrt{2} \cdot V_{MG1} \sin \omega t \quad (V) \quad (7)$$

Figure 9 shows the operation of the converter circuit when only M3 is on, M3 has a control pulse to open. The output voltage AC2 is equal to the voltage on L2 and on the M3. Energy is also charged to capacitor Cac2. In this scenario of transmitting energy from grid AC1 to grid AC2, the converter can adjust the voltage up or down to ensure that the output of the grid receives energy.

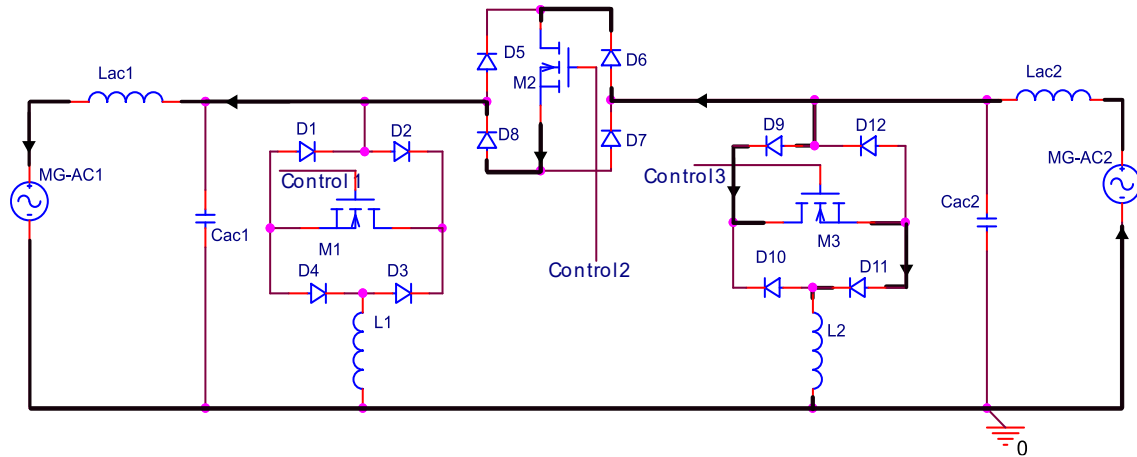


Figure 7. Status diagram of the converter operation when switches M2 and M3 are on at the same time

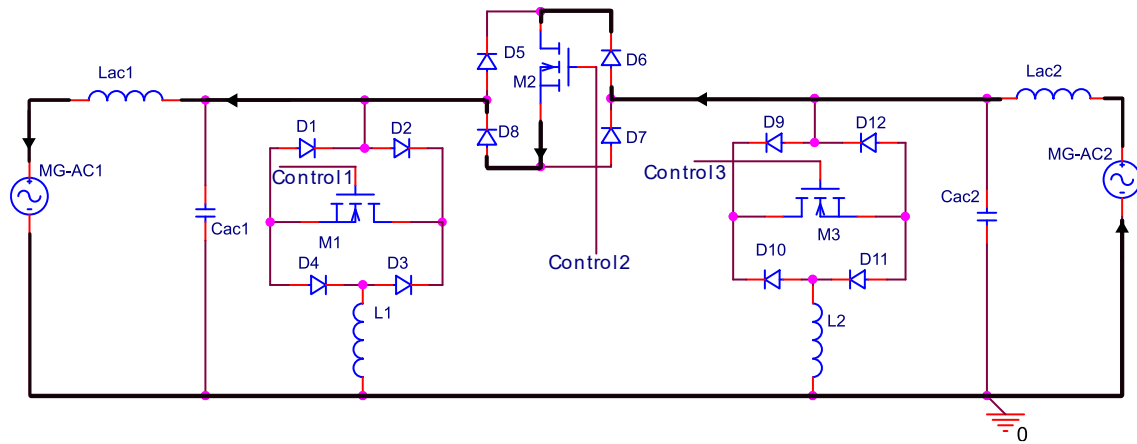


Figure 8. State diagram of converter operation when M2 switches are on ( $\pi-2\pi$ )

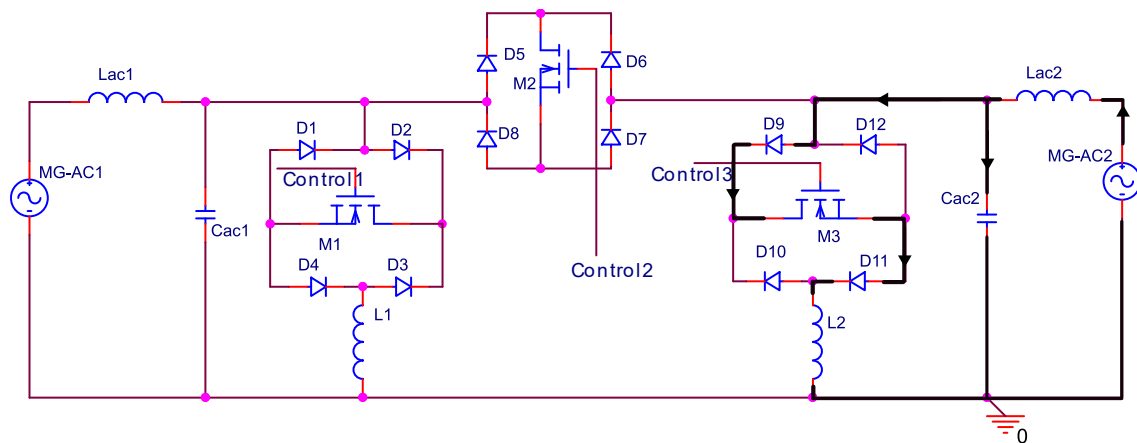


Figure 9. State diagram of converter operation when M3 are on

### 2.1.2. Scenario two

Like scenario 1 AC2-AC1 grid energy, in this scenario, there are similar modes and converter operations as AC1 to AC2 grid energy scenario with basic conditions. Grid-connected condition, using both load priority and AC microgrid renewable energy source working independently.

$$P_{loadAC1} > P_{PV1} + P_{win1} + P_{source-AC1} \quad (8)$$

In practice, the Ppv and Pwin sources fluctuate instantaneously in a value that requires compensation and energy consumption.

$$P_{loadAC1} > P_{win1} + P_{source-AC1} \quad (9)$$

Ppv stops generating electricity during off-peak hours, or when the bamboo is obscured by clouds.

$$P_{loadAC1} > P_{source-AC1} \quad (10)$$

Ppv and Pwin sources do not generate energy.

## 2.2. Cases where integration into the proposed AC/AC converter is possible

### 2.2.1. Scenario three

Scenario 3 is two grids supply energy to the storage system when the load of grid AC1 and grid AC2 decreases or the power source of the two grids increases, leading to excess energy from the two grids. At this time, the storage system is supplied (charged) with energy through AC/DC or AC/AC to AC/DC converters connected at the node of pins D of switches M1 and M3 in the power circuit converter as shown in Figure 2.

### 2.2.2. Scenario four

Scenario 4 is two microgrids AC1 and AC2 provide enough power for the load, the AC/AC converter does not operate, and the two grids work independently. In the power circuit, there must be two energy recovery circuits Dph1 and Cph1 to limit the voltage stress on M1 and M3. This circuit is connected to the D pole of M1 and M3 as shown in Figure 10. When the energy accumulated from the coils L1 and Cph1 during the period t1-t2 operates in the positive half cycle, the opening time of M1 ends at t2, the energy is transferred along the path L1-D3-Dph1-AC2 grid and Cph1-AC2 grid. Like recovery circuit 2 (Dph2 and Cph2) when operating in the negative half cycle. Figure 11 shows a recovery circuit solution to reduce the voltage stress on switches M1 and M3 in the converter. This is a suitable solution for the power circuit when the voltage stress signal on M1 is absent and there is a recovery circuit solution.

## 2.3. Proposed control mechanism for AC/AC converter

The control method in this converter is as follows: Adjust the voltage parameters. By adjusting the pulse width according to the PWM [26] modulation method as shown in Figure 12. The measured feedback signal is the voltage, frequency and phase angle parameters at the AC2 microgrid compared to the input signal from the AC1 grid, thereby providing control signals for the switches M1, M2, and M3 with the DC switching technology in the power circuit in Figure 2. Adjust the operating mode according to the power circuit design of the AC/AC unit as shown in Figure 12. According to the four main operating scenarios of the converter, there are six specific modes as analyzed above for scenario 1.

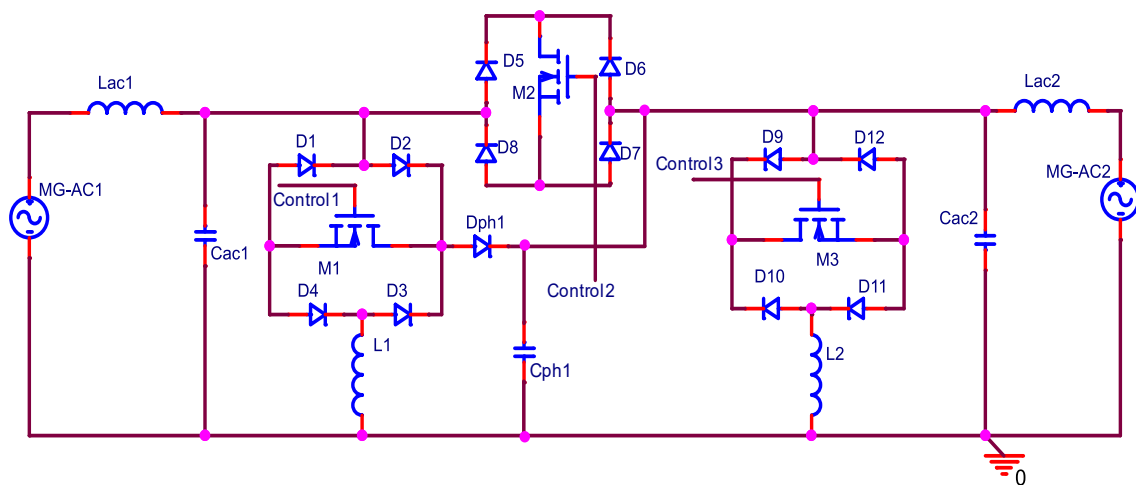


Figure 10. Voltage stress reduces the recovery circuit on M1

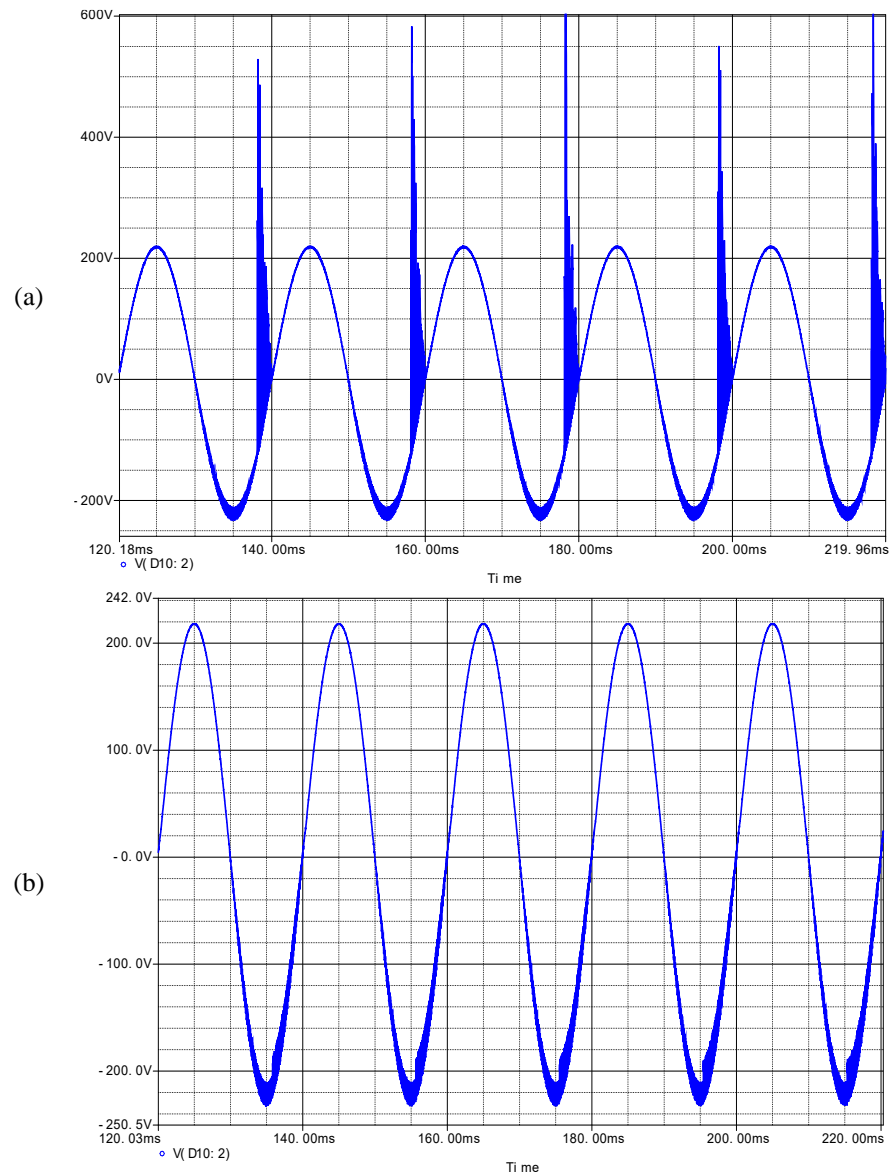


Figure 11. Circuit diagram comparing voltage values on M1 and M3 when there is a recovery circuit: (a) voltage on M1 without recovery circuit Dph1 & Cph1 and (b) voltage on M1 when there is recovery circuit Dph1 & Cph1

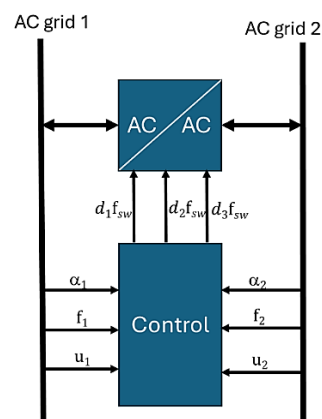


Figure 12. Block diagram of the overall control section of the AC/AC converter operation



### 3. SIMULATION RESULTS

The waveform conversion will be affected by parameters such as parasitic components in electronic elements; pulse width; values of passive elements in the power circuit; switching key, and switching frequency. The simulation part with different parameters: control frequency; pulse width M1, M3, M2; and load power value. Figures 13 and 14 show the input current and voltage signals (AC1 grid - corresponding to the I(ACmg1) and V(ACmg1) probes) and the output (AC2 grid - corresponding to the I(Rload) and V(Rload) probes). The average power measured at the input and output of the AC/AC converter is close to the value of 3-3.5 kW.

The output voltage amplitude value decreases by  $\pm 8.7$  V (THD = 3.9), when increasing the duty value of M1 and M2 to 75%, the output voltage amplitude decreases within the value of  $\pm 2.5$  V (THD) as shown in Figure 13. Thus, the THD parameter is within the allowable range and the pulse width can be adjusted accordingly because if the pulse width of M1 or M2 or both M1 and M2 is increased, it will affect the efficiency of the converter (it will reduce the efficiency) and the life of the switch. The current IEC standard is issued by the International Technical Committee International Electrotechnical Commission published.

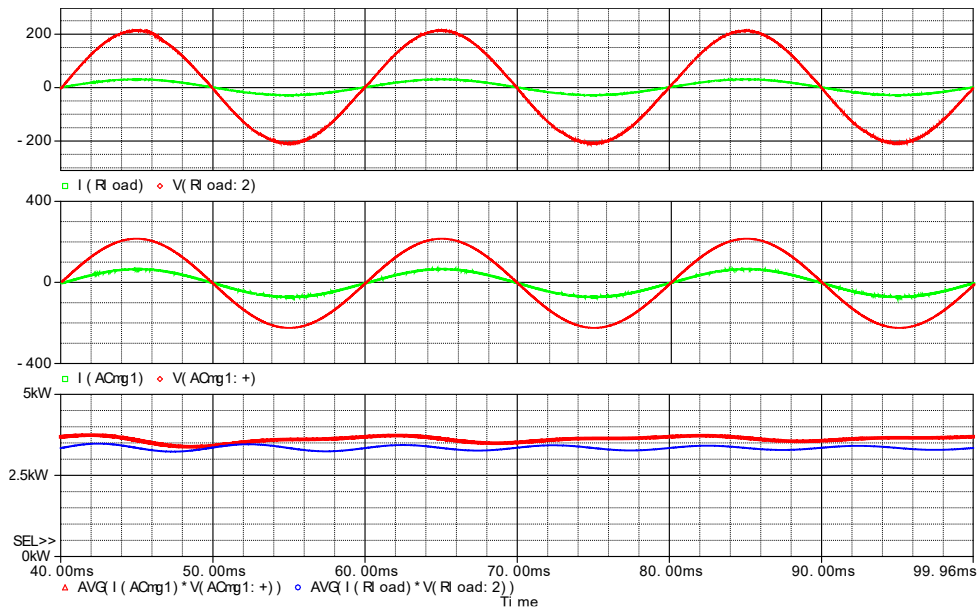


Figure 13. The 3.5 kW, duty M1 and M3 = 10%, duty M2 = 60%, frequency for switch = 30 kHz

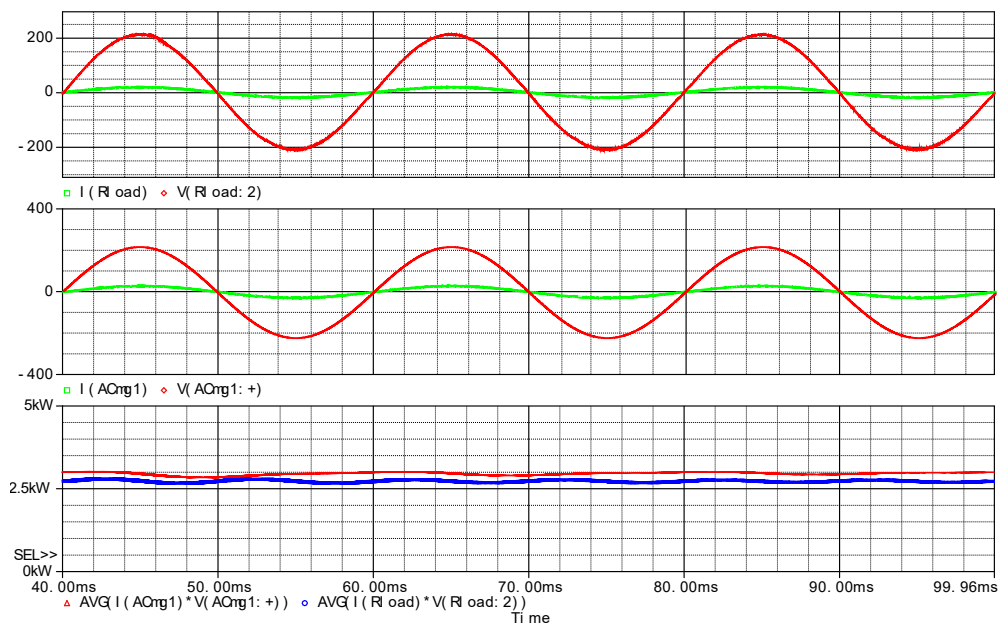


Figure 14. The 3 kW, duty M1 and M3 = 10%, duty M2 = 60%, frequency for switch = 30 kHz

Figure 15 shows the input and output voltage current signals of the converter, the average power value with the input parameters of the AC/AC converter with a capacity of 2.5 kW. With this input parameter, the converter operates well with a switching control frequency of 60 kHz. The output voltage amplitude value of AC grid 2 is reduced compared to AC grid 1 by  $\pm 6$  V. From here, we can adjust the frequency value, and the pulse width of the M1 and M2 switches to ensure that the voltage amplitude reaches the same value as the single-phase AC grid.

Figure 16 shows the input and output voltage current signals of the converter, the average power value with the input parameters of the AC/AC converter with a capacity of 2 kW. With this input parameter, the converter operates well with a switching control frequency of 30 kHz, the pulse width of the switches varies with the values M1 and M3 = 10%, M2 = 40%. The output voltage amplitude value of AC grid 2 is reduced compared to AC grid 1 by  $\pm 4$  V. From here, we can adjust the frequency value, and the pulse width of the M1 and M2 switches to ensure that the voltage amplitude reaches the same value as the single-phase AC grid. Figure 17 is like the case of the converter described in Figure 16. The input parameter adjusts the power with a value of 1.5 kW. The basic output voltage and current form do not change in total harmonic distortion when switching frequency and control pulse width M1 and M2 as shown in Figure 16.

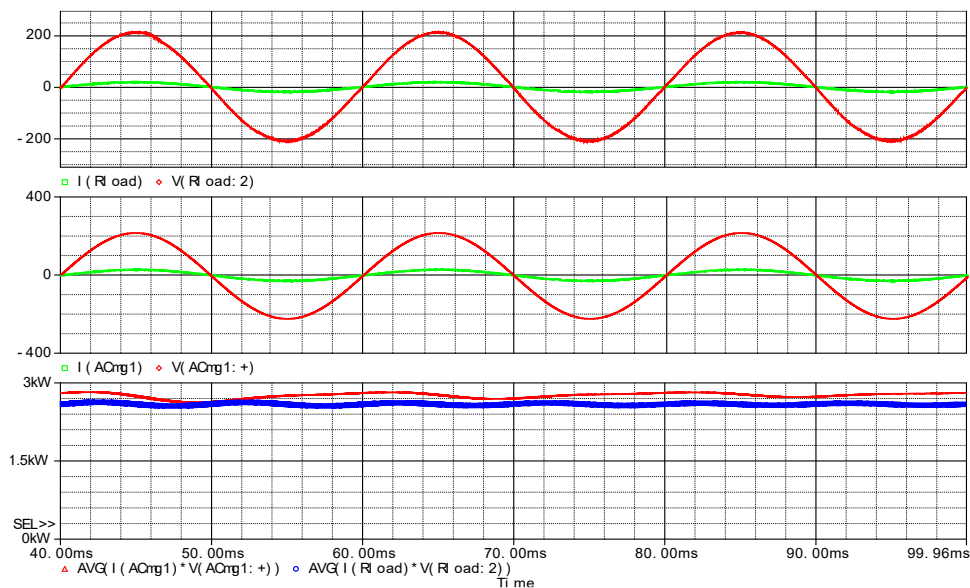


Figure 15. Circuit power 2.5 kW, duty M1 and M3 = 10%, duty M2 = 60%, frequency for switch = 30 kHz

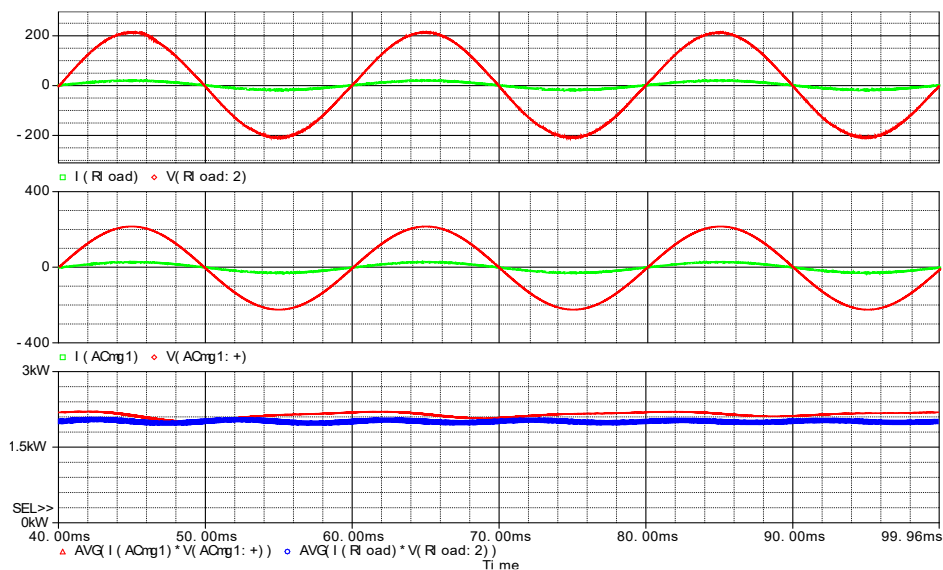


Figure 16. Power 2 kW, duty M1 and M3 = 10%, duty M2 = 40%, frequency for switch = 30 kHz

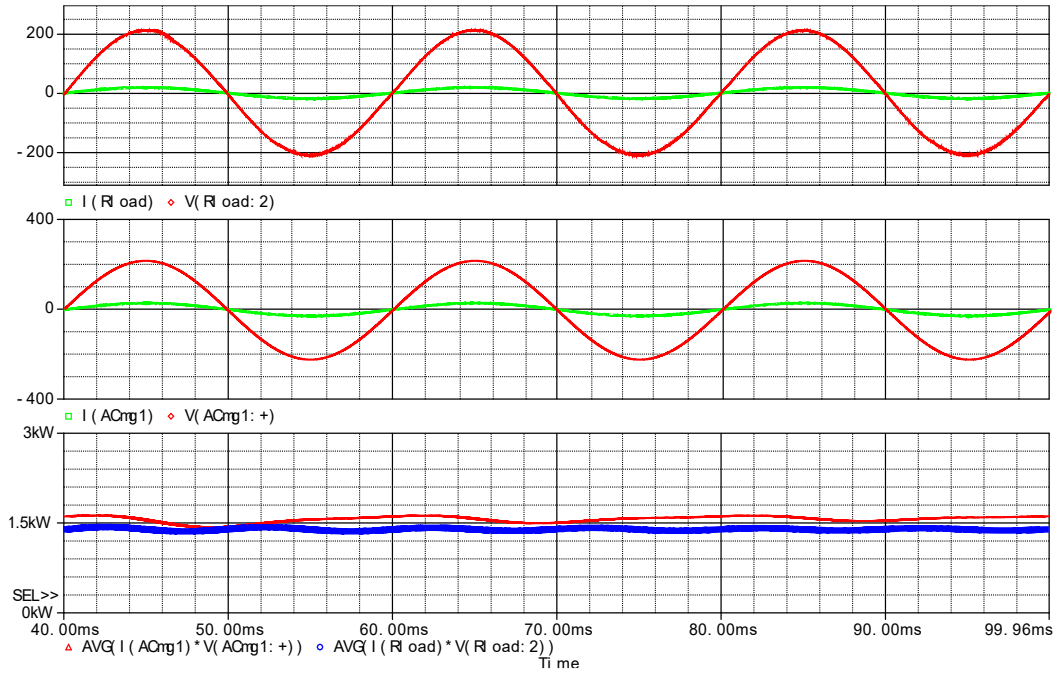


Figure 17. The 1.5 kW, duty M1 = 10%, duty M2 = 40%, frequency for switch = 30 kHz

Figure 18 shows the simulation results of the AC/AC converter with a load capacity on the AC2 grid of 1 kW, the input parameters are unchanged compared to Figure 17 and Figure 16. The power value, current, and voltage parameters are shown in Figure 18, Figure 19, and Figure 20 show different load cases on the AC2 grid from 100-500 W, the input and output parameters of the converter are described specifically in these figures. The output voltage amplitude on the load is almost equal to the input voltage, and the total harmonics of the output voltage signal are smaller than the cases working with higher power than the cases of 1.5-3 kW.

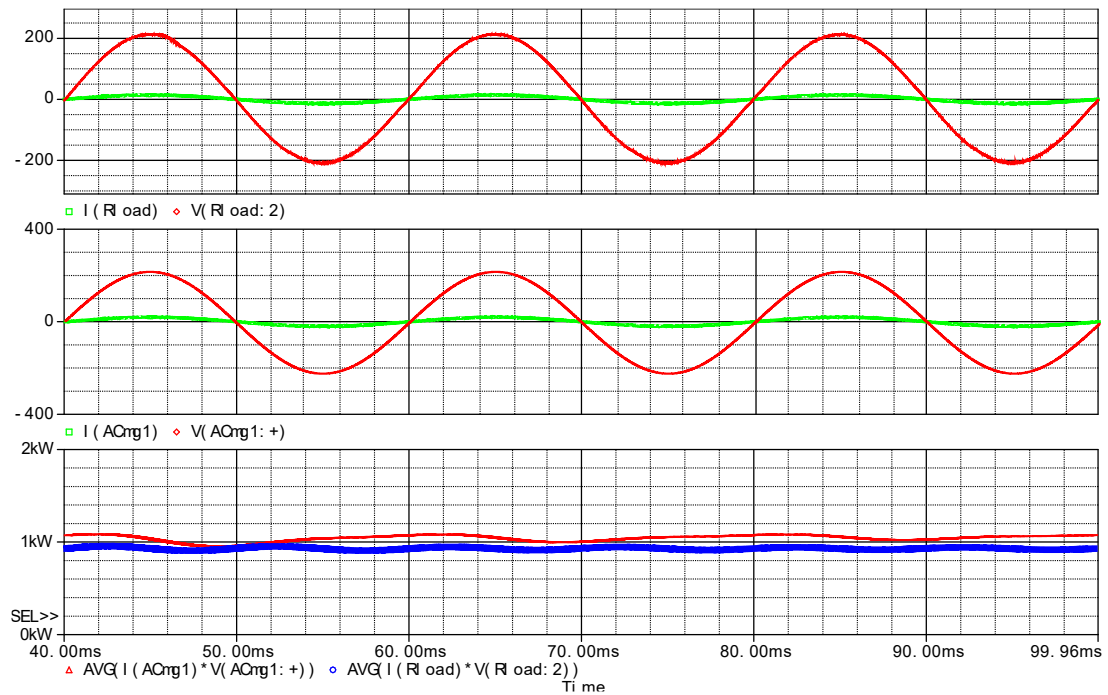


Figure 18. The 1 kW, duty M1 = 10%, duty M2 = 40%, frequency for switch = 40 kHz

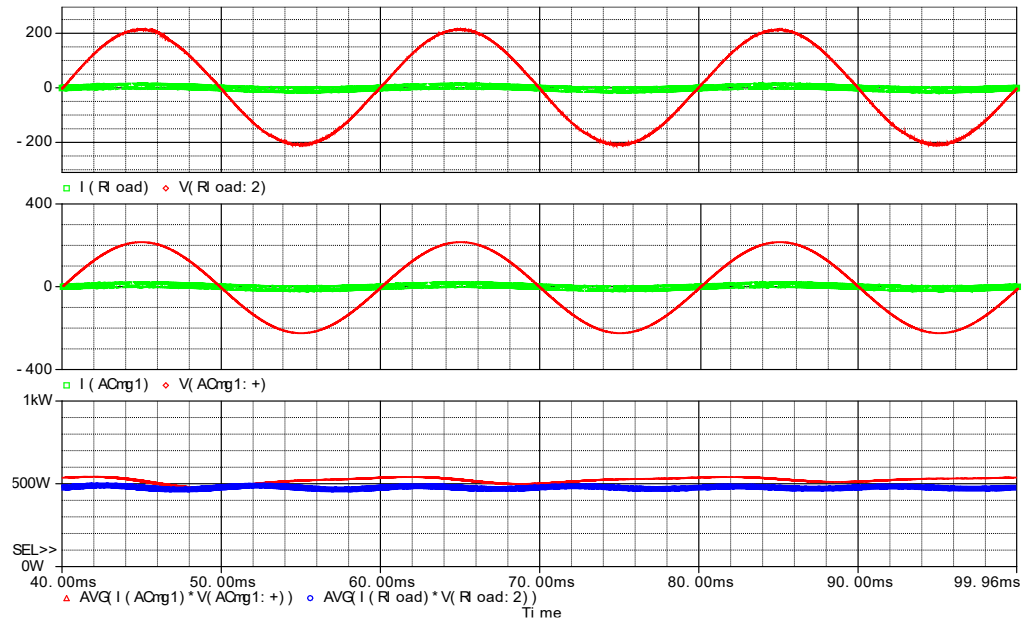


Figure 19. The 0.5 kW, duty M1=10%, duty M2 = 40%, frequency for switch = 30 kHz

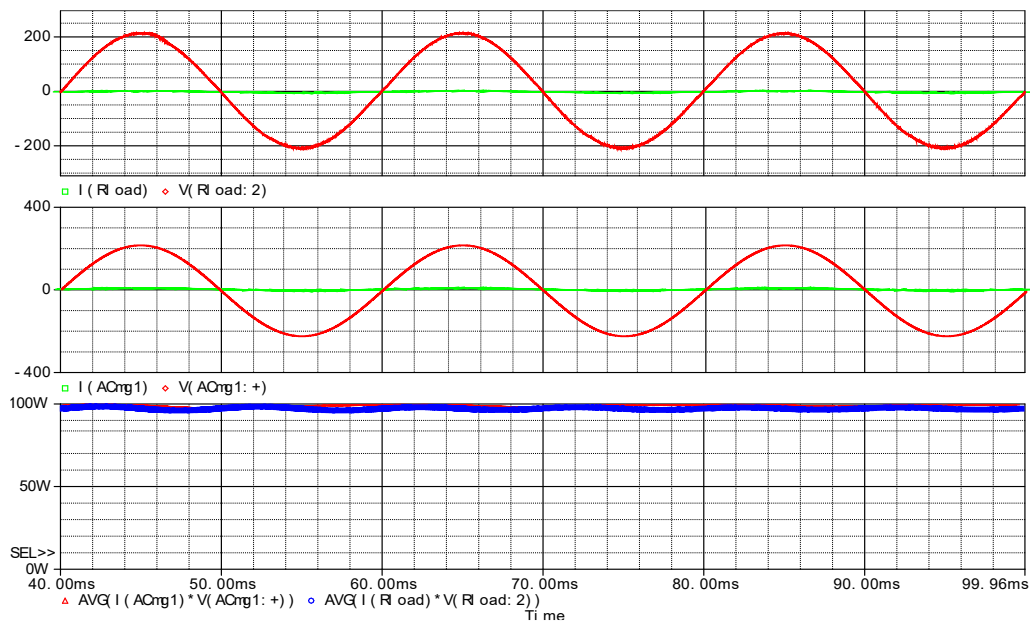


Figure 20. The 0.1 kW, duty M1 = 10%, duty M2 = 40%, frequency for switch = 30 kHz

The simulation performance is shown in the graph of Figure 21(a). The implementation method is the same as the case with different control frequencies of 5-100 kHz for electronic locks in the AC/AC converter. In the case of the switching frequency for the M1-M3 switch being 5 kHz, the AC/AC converter has the highest efficiency of 92.8% corresponding to the load capacity working at the AC2 grid of 100 W, the lowest efficiency of 89.2% corresponding to the load capacity of 3 kW. Similarly, with different switching frequency values in the increasing direction, the converter efficiency will increase gradually with the frequency value and the load capacity decreases. The highest frequency of 100 kHz with a load of 100 W has the maximum efficiency during the simulation of more than 96%. The low-frequency value of 30 kHz corresponds to the load capacity of 3 kW is 90.5%.

Figure 21(b) illustrates the influence of the control frequency on the harmonic distortion of the output voltage of the AC/AC converter corresponding to the switching frequency values of the power electronic

switch. The simulated power for the corresponding load value is 0.5-5 kW. In the simulation results, we see that with a large load power value of 5 kW, the total harmonic value is large and with a larger switching frequency, the total harmonic TDH (%) decreases.

In the specific analysis work, the pulse width ratio of M1 and M2 ( $d_2/d_1$ ) will affect the energy in the specific analysis work, the pulse width ratio of M1 and M2 ( $d_1/d_2$ ) will affect the energy conversion process, the value of the perfect component of the electronic power switches M1 and M2 in the scenario 1 of the converter. When adjusting the value of  $d_2/d_1$ , we see that the smaller this ratio is, the higher the efficiency of the converter in the simulation results is, such as 96.5% corresponding to  $d_1/d_2 = 0.25$ . And vice versa, if this ratio is larger, the efficiency will decrease by 90.5% with  $d_1/d_2 = 4$ , as shown in Figure 22.

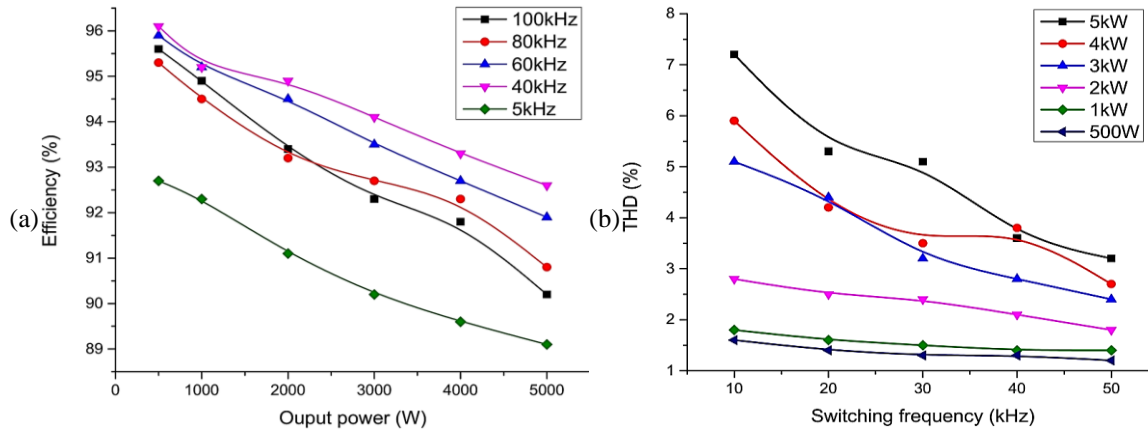


Figure 21. Simulation results of (a) performance with load power parameters and control frequency of AC/AC unit and (b) graph of the influence of control frequency and load on harmonic distortion of voltage THD

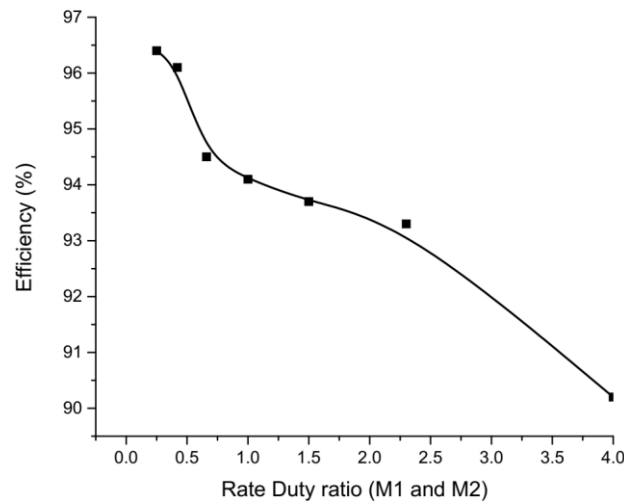


Figure 22. Pulse width parameter ratio for M1 and M2

#### 4. EXPERIMENTAL RESULTS

Figure 23(a) shows the system between two microgrids AC1 and AC2 transmitting energy from grid AC1 to grid AC2. The converter shows two basic components: the power circuit and the control circuit. The input and output circuit parameters, and control signals, are measured by multimeters, power, and oscilloscopes described in Figure 23(a). The model is implemented in the design laboratory. The load of grid AC1 is a hair dryer and a light bulb with a capacity ranging from 0.5-3.5 kW. Figure 23(b) shows the meter parameters for the AC/AC converter when transmitting power from the AC1 to the AC2 grid, the voltage measurement parameters at the AC1 grid, AC2 grid, and the power. For example, the load power is more than 1 kW with the load at the AC2 grid.



Table 1 shows the parameters of the power circuit elements of the converter, the measuring equipment needs to measure the experimental parameters for calculation and testing. Figure 24 shows the voltage curve on the power switches M1 shown in Figure 24(a) and M2 in Figure 24(b) operating in the circuit at scenario 1 with the load power at the AC2 microgrid being 1 kW. The M1 pulse width is 10% and the M2 pulse width is 80%, the switching frequency is 30 kHz.

The control signals for the switches M1 (yellow signal) and M2 (blue line signal) are shown in Figure 25(a). Figure 25(b) shows the AC1 grid voltage (yellow) and the AC2 grid load voltage (blue). The output voltage waveform has the amplitude of the single-phase AC grid voltage response. In Figure 26, the input and output voltage signals of the AC/AC converter circuit with a power transmission capacity of 1 kW as in Figure 26(a) and 1.5 W in Figure 26(b) are described. The yellow signal is the AC1 input voltage of the converter, the blue signal is the output voltage of the converter and to the load and grid AC2.

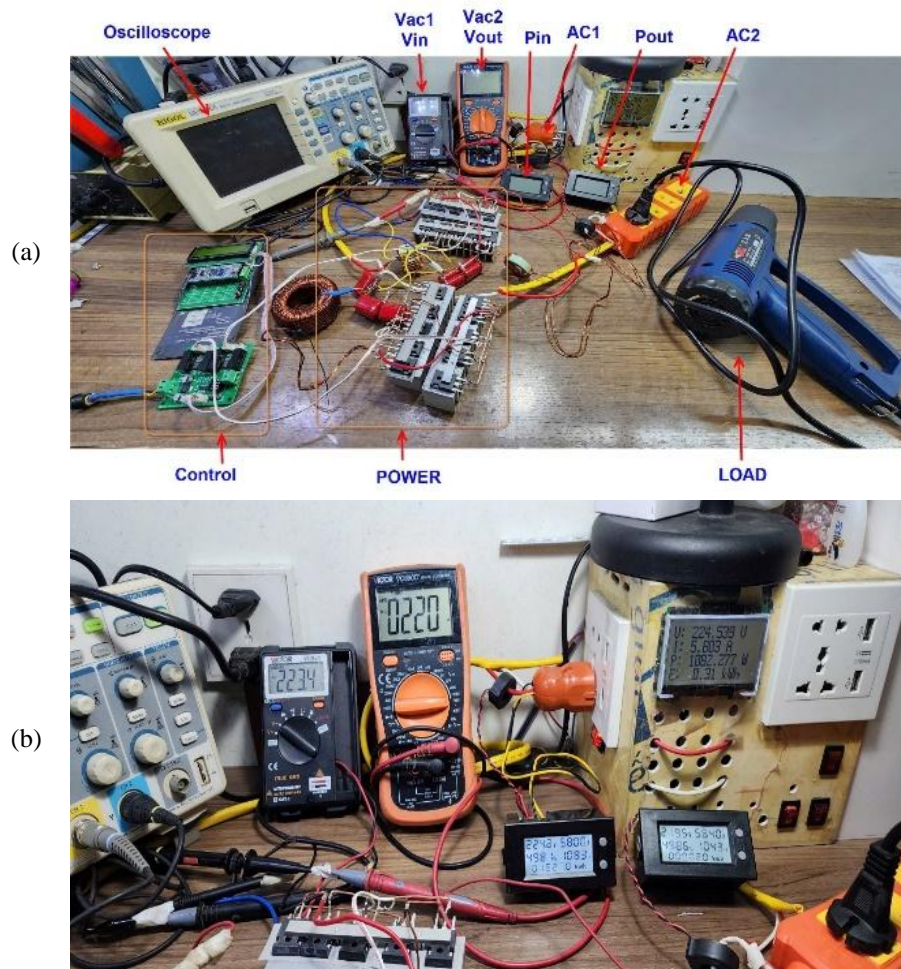


Figure 23. Image depicting laboratory experiment (a) image of AC/AC converter in the laboratory and (b) experimental measurement of the operating parameters of the proposed AC/AC converter

Table 1. Experimental parameters

Equipment	Parameter	Equipment	Parameter
Oscilloscope	300 Mhz, 2 Channel	Load3	Electric oven Comet CM6510, 1000 W
Voltage AC1 grid	220 VAC	M1, M2, M3	IPW65R041CFD 650 V 68.5 A
Voltage AC2 grid	220 VAC	D1 – D12	IDW75E60, 75 A 600 V, fast switching diode
Power meter AV69Z	VAC = 80-300 V, I-ACmax = 100 A	L <sub>AC1</sub> , L <sub>AC2</sub>	20 uH/50 A
Load1	Talon TH8623S – 2000 W	C <sub>AC1</sub> , C <sub>AC2</sub>	2.2 uF/1200 V (4×CB22 225 J 630 V)
Load2	Kettle – 1500 W	L1, L2	50 mH/50 A

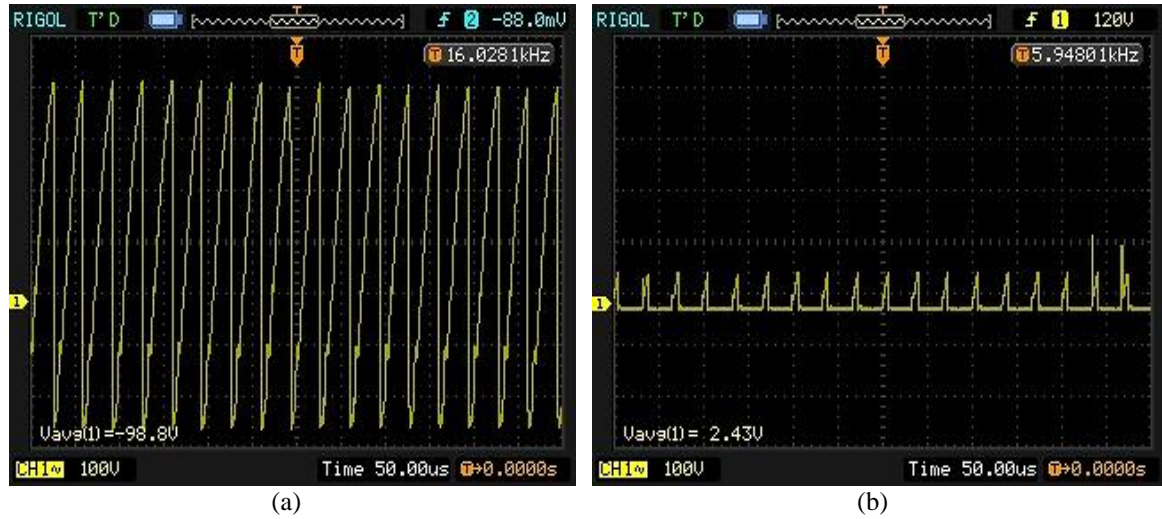


Figure 24. Voltage graph on the switch: (a) switch M1 and (b) circuit switch M2

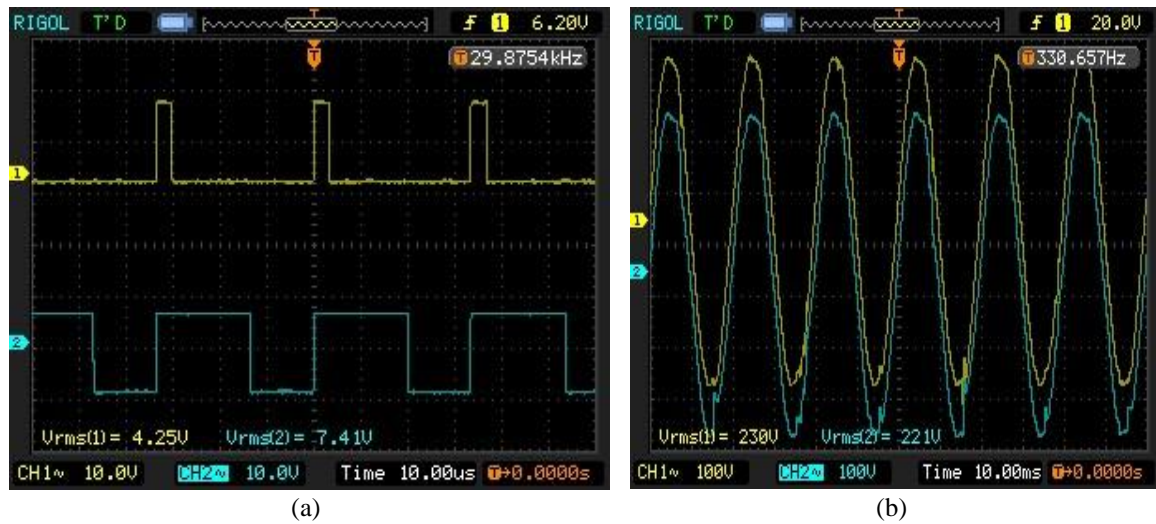


Figure 25. Voltage graphs of (a) control pulse signals M1 and M2 in the AC/AC converter circuit and (b) grid voltage form AC1 and AC2 with 0.5 kW transmission power

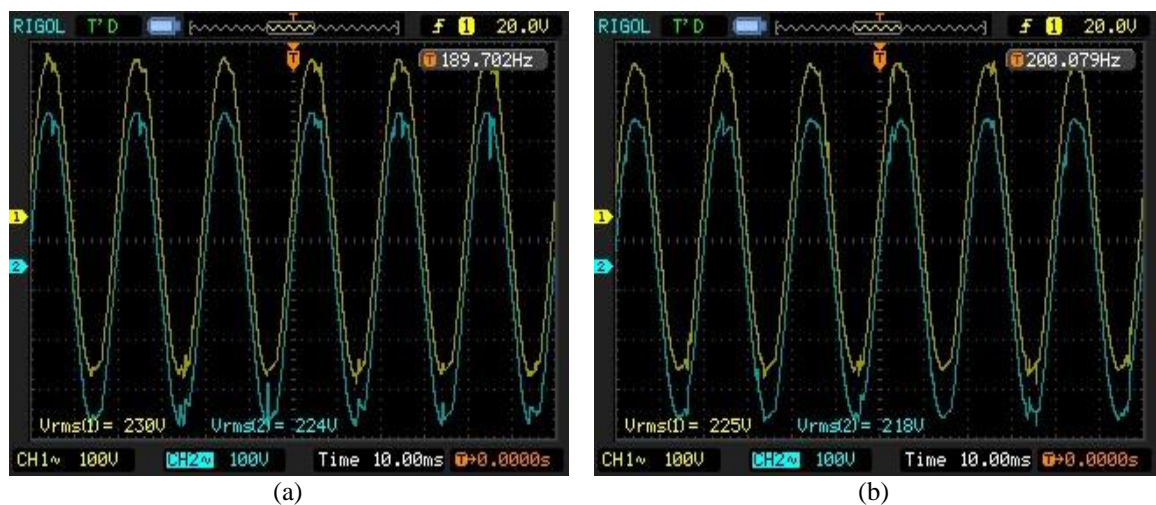


Figure 26. AC1 and AC2 grid voltage graph with transmission power of (a) 1 kW and (b) 1.5 kW



In Figures 27 and 28, the input and output voltage signals of the AC/AC converter circuit with a power transmission capacity of 2 kW as shown in Figure 27(a), and 2.5 kW are shown in Figure 27(b). Figure 28(a) with a power transmission capacity of 3 kW and Figure 28(b) is 3.5 kW. The yellow signal is the input voltage AC1 of the converter, the blue signal is the output voltage of the converter and to the load and grid AC2.

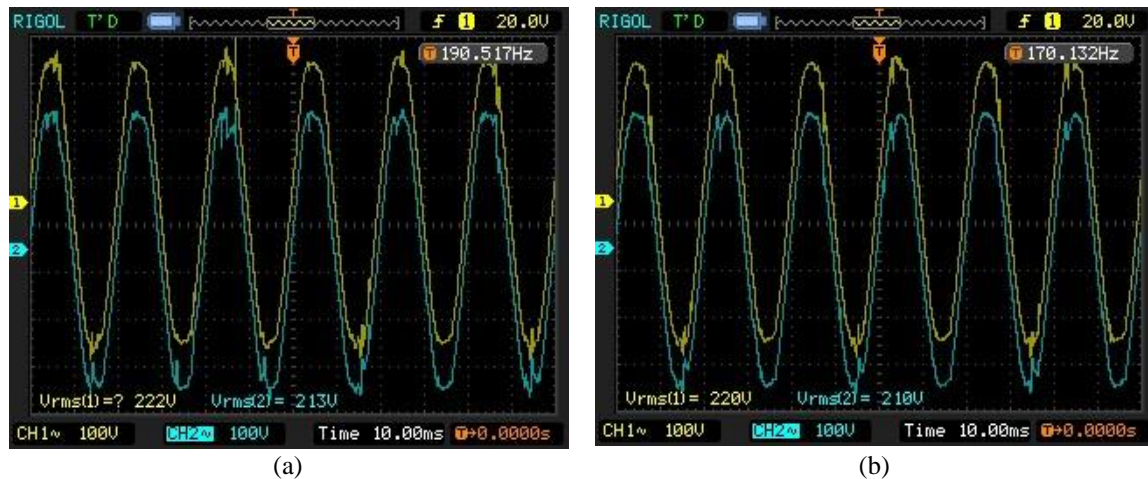


Figure 27. Grid voltage graph AC1 and AC2 with transmission power (a) 2 kW and (b) 2.5 kW

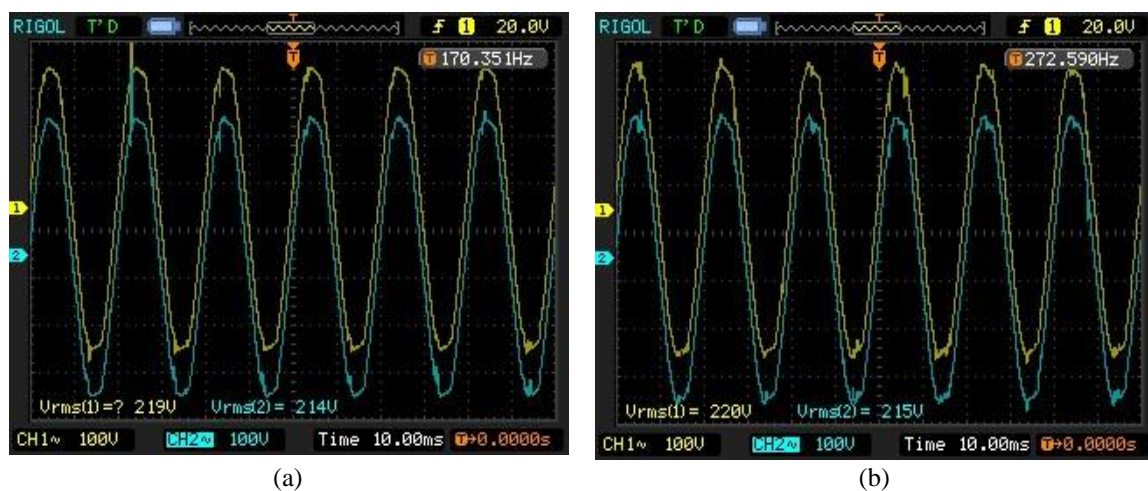


Figure 28. Grid voltage graph AC1 and AC2 with transmission power (a) 3 kW and (b) 3.5 kW

The performance comparison of simulation, experimental, and reference results for the proposed AC/AC converter is shown in Figure 29. The basic simulation values are shown by some ideal parameters such as conductors, main switches (MOSFET) and auxiliary (diodes), and coils in the power circuit, while the experimental part shows the actual values in the circuit with actual components and devices with some non-ideal parameters, so there is an error between the two experimental and simulation parts, the average efficiency of the converter is 0.5%. The experimental results of the proposed AC/AC converter show higher basic efficiency than the literature [15] at power values from 0.5-3.5 kW. In the proposed converter, the basic solution for the simple device power circuit has 3 main switches operating the conversion and transmitting energy in two directions directly, leading to the control circuit will be simple for the management and operation of the energy exchange process, the experimental conversion capacity is up to 3.5 kW [10], [11]. The voltage value on the main switch is limited by the energy recovery circuit and current stabilization by two coils L1 and L2, leading to reduced loss on the switch and increased efficiency in the converter.



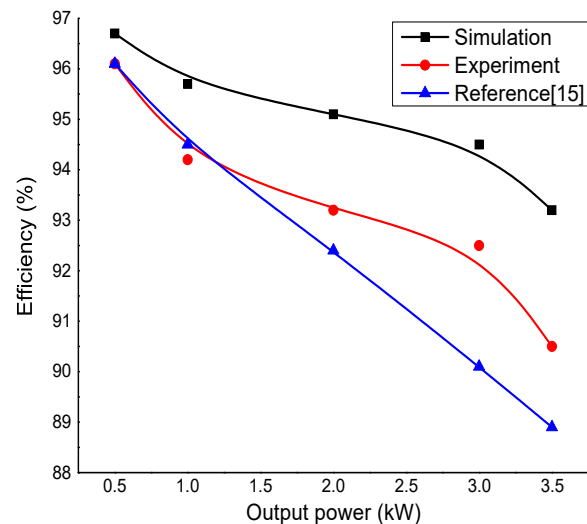


Figure 29. Comparison of converter performance with references

## 5. CONCLUSION

In this paper, an AC/AC converter that steps up or down the voltage to directly transfer energy between two AC microgrids is proposed. The proposed converter uses a minimum number of main switches and passive components to reduce the power loss of the converter and achieve high efficiency. It can be operated by simple SPWM control and does not require soft-switching controls. It does not suffer from switching and cross-over problems of the input source. Furthermore, it provides both constant input and output current. A comparison of the performance of the proposed converter with existing similar converters is presented. In addition, detailed circuit analysis, component design guidelines, and simulation results using the OrCAD environment are also presented. A laboratory prototype was built and tested to validate the performance of the converter and confirm the obtained results with measured and calculated values such as 96.3% efficiency at 0.5 kW and 90.8% efficiency at 3.5 kW. The system can connect to the storage system to make the energy usage and energy storage between AC microgrids more flexible. Compared with the traditional AC/AC converter, it has more reliability and flexibility in the operation of AC microgrids in the current power system. Moreover, the pulse width value of the M1 and M3 switches works with a small value, so the efficiency of the converter is improved.

## ACKNOWLEDGEMENTS

The research team would like to thank the Posts and Telecommunications Institute of Technology Hanoi, Vietnam and Hanoi University of Industry for creating favorable conditions during the implementation of the research content of this article.




## REFERENCES

- [1] H. Khajeh, A. Akbari Foroud, and H. Firoozi, "Robust bidding strategies and scheduling of a price-maker microgrid aggregator participating in a pool-based electricity market," *IET Generation, Transmission & Distribution*, vol. 13, no. 4, pp. 468–477, Feb. 2019, doi: 10.1049/iet-gtd.2018.5061.
- [2] T. A. Nguyen and M. L. Crow, "Stochastic optimization of renewable-based microgrid operation incorporating battery operating cost," *IEEE Transactions on Power Systems*, vol. 31, no. 3, pp. 2289–2296, May 2016, doi: 10.1109/TPWRS.2015.2455491.
- [3] S. Fattaheian-Dehkordi, M. Tavakkoli, A. Abbaspour, M. Fotuhi-Firuzabad, and M. Lehtonen, "Distribution grid flexibility-ramp minimization using local resources," in *2019 IEEE PES Innovative Smart Grid Technologies Europe (ISGT-Europe)*, 2019, pp. 1–5, doi: 10.1109/ISGTEurope.2019.8905754.
- [4] S. Fattaheian-Dehkordi, A. Rajaei, A. Abbaspour, M. Fotuhi-Firuzabad, and M. Lehtonen, "Distributed transactive framework for congestion management of multiple-microgrid distribution systems," *IEEE Transactions on Smart Grid*, vol. 13, no. 2, pp. 1335–1346, Mar. 2022, doi: 10.1109/TSG.2021.3135139.
- [5] B. Singh, P. Jayaprakash, and D. P. Kothari, "New control approach for capacitor supported DSTATCOM in three-phase four wire distribution system under non-ideal supply voltage conditions based on synchronous reference frame theory," *International Journal of Electrical Power & Energy Systems*, vol. 33, no. 5, pp. 1109–1117, Jun. 2011, doi: 10.1016/j.ijepes.2010.12.006.
- [6] A. Javadi, A. Hamadi, L. Woodward, and K. Al-Haddad, "Experimental investigation on a hybrid series active power compensator to improve power quality of typical households," *IEEE Transactions on Industrial Electronics*, pp. 1–1, 2016, doi: 10.1109/TIE.2016.2546848.
- [7] R. Langella, A. Testa, and E. Alii, "IEEE recommended practice and requirements for harmonic control in electric power systems," in *IEEE recommended practice*, IEEE, 2014.




- [8] A. Mohamed, M. Elshaer, and O. Mohammed, "Bi-directional AC-DC/DC-AC converter for power sharing of hybrid AC/DC systems," in *2011 IEEE Power and Energy Society General Meeting*, IEEE, Jul. 2011, pp. 1–8. doi: 10.1109/PES.2011.6039868.
- [9] A. Ghosh and G. Ledwich, "Power quality enhancement using custom power devices," in *Power Electronics and Power Systems (PEPS)*, Springer Science+Business Media, LLC, 2002, doi: 10.1007/978-1-4615-1153-3.
- [10] S. Subramanian and M. K. Mishra, "Interphase AC-AC topology for voltage sag supporter," *IEEE Transactions on Power Electronics*, vol. 25, no. 2, pp. 514–518, Feb. 2010, doi: 10.1109/TPEL.2009.2027601.
- [11] S. Sharifi, M. Monfared, M. Babaei, and A. Pourfaraj, "Highly efficient single-phase Buck-Boost variable-frequency AC-AC converter with inherent commutation capability," *IEEE Transactions on Industrial Electronics*, vol. 67, no. 5, pp. 3640–3649, May 2020, doi: 10.1109/TIE.2019.2914644.
- [12] K. Ma, H. Ma, H. Zheng, and Z. Bo, "Modeling and control of a mutual support hybrid AC/DC micro-grid," in *2017 China International Electrical and Energy Conference (CIEEC)*, 2017, pp. 510–514, doi: 10.1109/CIEEC.2017.8388500.
- [13] H. Zeng, H. Zhao, and Q. Yang, "Coordinated energy management in autonomous hybrid AC/DC microgrids," in *2014 International Conference on Power System Technology*, IEEE, Oct. 2014, pp. 3186–3193. doi: 10.1109/POWERCON.2014.6993710.
- [14] P. Szczesniak, "Challenges and design requirements for industrial applications of AC/AC power converters without DC-link," *Energies*, vol. 12, no. 8, p. 1581, Apr. 2019, doi: 10.3390/en12081581.
- [15] H. Sarnago, A. Mediano, and Ó. Lucia, "High efficiency AC-AC power electronic converter applied to domestic induction heating," *IEEE Transactions on Power Electronics*, vol. 27, no. 8, pp. 3676–3684, Aug. 2012, doi: 10.1109/TPEL.2012.2185067.
- [16] H. F. Ahmed, H. Cha, A. A. Khan, and H.-G. Kim, "A highly reliable single-phase high-frequency isolated double step-down AC-AC converter with both noninverting and inverting operations," *IEEE Transactions on Industry Applications*, vol. 52, no. 6, pp. 4878–4887, Nov. 2016, doi: 10.1109/TIA.2016.2592466.
- [17] F. L. Luo and H. Ye, "DC-modulated power factor correction AC/AC converters," in *2007 2nd IEEE Conference on Industrial Electronics and Applications*, IEEE, May 2007, pp. 1477–1483, doi: 10.1109/ICIEA.2007.4318652.
- [18] M. S. Bakar, N. A. Ibrahim, and A. Z. Ahmad, "Total harmonic distortion study for improvement of AC-AC converter under Buck-type," in *Advances in Intelligent Manufacturing and Mechatronics*, 2023, pp. 305–311, doi: 10.1007/978-981-19-8703-8\_26.
- [19] D. Stanelyte and V. Radziukynas, "Review of voltage and reactive power control algorithms in electrical distribution networks," *Energies*, vol. 13, no. 1, p. 58, Dec. 2019, doi: 10.3390/en13010058.
- [20] L. Zhang and T. S. Sidhu, "New dynamic voltage and reactive power control method for distribution networks with DG integration," in *2014 IEEE Electrical Power and Energy Conference*, IEEE, Nov. 2014, pp. 190–195, doi: 10.1109/EPEC.2014.39.
- [21] R. K. Rojin, "A review of power quality problems and solutions in electrical power system," *International Journal of Advanced Research in Electrical, Electronics and Instrumentation Engineering*, vol. 2, no. 11, pp. 5605–5614, 2013.
- [22] EREA and DEA, "Viet Nam Energy Outlook Report 2021," 2022. [Online]. Available: <http://vepg.vn/wp-content/uploads/2022/06/Vietnam-Energy-Outlook-Report-2021-English.pdf>
- [23] B. S. Hartono, Budiyo, and R. Setiabudy, "Review of microgrid technology," in *2013 International Conference on QiR*, IEEE, Jun. 2013, pp. 127–132, doi: 10.1109/QiR.2013.6632550.
- [24] J. J. Justo, F. Mwasilu, J. Lee, and J.-W. Jung, "AC-microgrids versus DC-microgrids with distributed energy resources: A review," *Renewable and Sustainable Energy Reviews*, vol. 24, pp. 387–405, Aug. 2013, doi: 10.1016/j.rser.2013.03.067.
- [25] "The National Assembly hereby promulgates the law on import and export duty." [Online]. Available: [https://www.economica.vn/Content/files/LAW %26 REG/107\\_2015\\_QH13 Law on Import Export Duties.pdf](https://www.economica.vn/Content/files/LAW%20REG/107_2015_QH13%20Law%20on%20Import%20Export%20Duties.pdf)
- [26] D.-C. Lee and Y.-S. Kim, "Control of single-phase-to-three-phase AC/DC/AC PWM converters for induction motor drives," *IEEE Transactions on Industrial Electronics*, vol. 54, no. 2, pp. 797–804, Apr. 2007, doi: 10.1109/TIE.2007.891780.

## BIOGRAPHIES OF AUTHORS



**Nguyen The Vinh**    is a lecturer at the Faculty of Electronic Engineering I, Posts and Telecommunications Institute of Technology (PTIT), Hanoi, Vietnam. He graduated in 2001 with a degree in Electrification from Thai Nguyen University of Technology, Vietnam. In 2008, he completed a Master's degree in Electrical Equipment, Networks, and Power Plants from Thai Nguyen University. He obtained his Ph.D. in Electrical Engineering from the University of Lorraine, France, in 2014. He is head of renewable energy and environmental research group. His research interests include the field of digital design, industrial applications, industrial electronics, industrial informatics, power electronics, renewable energy, embedded system, artificial intelligence, intelligent control, and embedded system for environmental measurement. He can be contacted at email: [vinhnt@ptit.edu.vn](mailto:vinhnt@ptit.edu.vn).



**Nguyen Van Dung**    was born in Vinh Phuc, Vietnam. He received the B.S. and M.S. degrees in Electronics Engineering from the Hanoi University of Industry (HaUI), Hanoi, Vietnam, in 2009 and 2018. He is currently a Lecturer at Faculty of Electronic Engineering in HaUI. His research interests include control of power electronics, control of electric drivers, smart grids, smart home, and automatic control system. He can be contacted at email: [dungnv@haui.edu.vn](mailto:dungnv@haui.edu.vn).